JOURNAL OF AIRCRAFT
Vol. 32, No. 5, September–October 1995

Vortex Asymmetry and Induced Side Forces on Elliptic Cones at High Incidence

P. R. Viswanath*
National Aerospace Laboratories, Bangalore 560 017, India

Experimental studies were carried out investigating features of vortex asymmetry and induced side forces on a family of three elliptic cones at subsonic speeds. Measurements of forces, moments, and surface flow visualization studies were made up to an angle of attack of 45 deg over a wide range of Reynolds number. Results show that ellipticity progressively reduces the angle of attack for the onset of side force up to an ellipticity ratio (defined here as the ratio of major to minor axis) of 1.43, beyond which there is a reversal in this trend for both horizontal as well as vertical orientations of the ellipse. Interestingly, the (maximum) side force magnitudes are larger for the horizontal compared to the vertical ellipse orientation on each model. A correlation of the angle of attack for the onset of asymmetry on pointed forebodies with elliptic cross section is suggested. These results provide strong support to the hypothesis (often made in the literature) that inviscid mechanisms may play a key role in triggering asymmetry of vortex flows.

Nomenclature

A = reference base area, area of a circle with planform width at the base of the elliptic cone as diameter
A_S = side area of elliptic cone
C_N = normal force coefficient, normal force/$(q_\infty A)$
C_S = side force coefficient, side force/$(q_\infty A)$
C_S^* = side force coefficient based on side area, side force/$(q_\infty A_S)$
D = planform width of the elliptic cone at the base (Fig. 1)
H = height of the elliptic cone at the base (Fig. 1)
M_∞ = freestream Mach number
q_∞ = freestream dynamic pressure
Re = unit Reynolds number based on freestream conditions
Re_D = Reynolds number based on freestream conditions and D
U_c = crossflow velocity
α = angle of attack
α_0 = angle of attack for onset of side force
ε = ellipticity ratio, ratio of major to minor diameter of elliptic cone
θ_c = planform (nose) semiapex angle
λ = D/H, Fig. 1
φ = roll angle
ψ = crossflow separation angle, Fig. 8

I. Introduction

THE problem of vortex asymmetry and the associated side forces (and yawing moments) on pointed forebodies at high angles of attack and zero sideslip has received considerable attention in the literature.[1-3] Our broad knowledge of this flow involving vortex asymmetry has been a result of extensive experimental research on axisymmetric configurations during the last 15 years, which have revealed the important parameters affecting the onset of vortex asymmetry and the magnitude of induced side forces; the primary geometrical parameters are the nose apex angle, forebody cross-sectional shape, and fineness ratio. Several papers in the literature have focused attention on the cause of asymmetry and have attempted to provide explanations based largely on inviscid arguments.[4-6] Keener and Chapman,[4] by comparing the similarities between asymmetric flows on bodies and slender, sharp delta wings (which have symmetric separation lines), suggested that asymmetry may occur due to the hydrodynamic instability of symmetric vortex flows. Some of the recent computational studies[7-9] employing time-dependent, Reynolds-averaged, thin-layer Navier–Stokes equations have attempted to provide insight towards understanding this complex phenomenon. Excellent reviews on the subject have been written[1-3,10-12]; the problem is still intractable to modeling and prediction, even in an engineering sense.

Since the vortex flows developing on the forebody depend strongly on the cross-sectional shape, one can expect significant effects on vortex asymmetry and the side forces generated as well. In the context of fighter aircraft, forebody cross section is rarely circular and perhaps not even made up of sheared circles. Elliptic (or ellipse-like) cross sections are relevant to both aircraft and missile applications and the associated aerodynamic benefits have been amply demonstrated[13-16]; e.g., a flattened or horizontal ellipse can offer increased directional stability under high-alpha conditions, in addition to better normal force characteristics. Surprisingly, the available data in the literature related to asymmetry on forebodies (and on slender bodies) with elliptic cross section is rather meager, despite the current technological interest[15,16]; the paucity of data, in particular, with regard to Reynolds number effects, has been stressed by Polhamus.[17] The experimental studies of Keener et al.,[18] which included a tangent ogive forebody with a 1.43:1 ellipse, showed an earlier onset of asymmetry for both horizontal and vertical ellipse orientations and side forces comparable to the axisymmetric counterpart. Roos and Kegelman[19] presented results of aerodynamic characteristics on three forebodies up to high angles of attack, which included a horizontal ellipse as well and a chine; the forebody with elliptic cross section was geometrically similar to that employed by Keener et al.[18] and showed an earlier onset compared to a circular cone of the same nose apex angle. A recent study of Lowson and Ponton[20] included two cones with 2:1 and 3:1 ellipses, but data on the onset of asymmetry or side forces were not reported in the paper; the authors, based on flow visualization experiments on the cones with horizontal ellipse orientation, pointed out that the asymmetry was probably linked to vortex breakdown on these two bodies.

Received June 11, 1994; revision received March 6, 1995; accepted for publication March 6, 1995.

*Deputy Head, Experimental Aerodynamics Division. Associate Fellow AIAA.

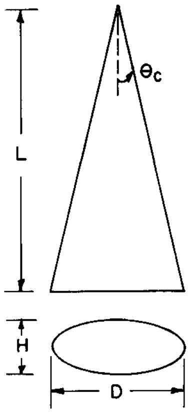

Model	ε	L mm	λ	θ_c°	D mm
EC1	1.10	360	1.10	10	127
			0.91	9.1	115
EC2	1.50	426	1.50	12	181
			0.66	8	120
EC3	2.0	413	2.0	12	175
			0.5	6	87

$\lambda = D/H$

Fig. 1 Geometric details of cone models.

The present study was motivated by the need to provide a broad understanding of the features associated with vortex asymmetry and side force generation on pointed forebodies of elliptic cross section. Experiments have been performed on three elliptic cones at subsonic speeds over a reasonable range of Reynolds number and covering angles of attack up to 45 deg. Results of the onset of vortex asymmetry, side force characteristics, and surface flow features on the leeside are discussed in detail; a correlation for the onset of vortex asymmetry has also been suggested.

II. Experiments

Wind-tunnel tests on three elliptic cones were conducted in the 1.2-m trisonic blowdown facility; the solid wall test section was utilized up to a freestream Mach number of 0.4, and for limited tests at higher Mach numbers, the transonic (perforated) test section was used.

The geometric details of all three elliptic cones having ellipticity ratios ε of 1.1, 1.5, and 2.0, respectively, are given in Fig. 1. The term ellipticity ratio (ratio of major to minor axis) is used here in a general sense to characterize a given elliptic cone. The ratio of planform width-to-height λ defines the ellipse orientation as well (Fig. 1); $\lambda > 1$ refers to a horizontal ellipse (HE), and $\lambda < 1$ refers to a vertical ellipse (VE) orientation. The cone models, made of high-strength steel, were fabricated on a numerically controlled milling machine and finished accurately using two-dimensional templates.

Six-component balance measurements on the models, for both horizontal and vertical ellipse orientations, were made using a 37.5-mm Able balance. The model incidence range of 0–45 deg was covered in two steps; with the normal pitch system in the range 0–25 deg and with a high alpha attachment (having a preset incidence of 25 deg) coupled to the tunnel pitch system to cover 20–45 deg, providing an overlap of 5 deg. Extensive surface flow visualization studies were carried out using titanium dioxide in vacuum pump oil and oleic acid. For each model, Reynolds number range was obtained by varying the freestream Mach number in the range of 0.20–0.40 and the tunnel stagnation pressure.

Uncertainty in the measured side force coefficient C_S, estimated using the method of Kline and McClintock[21] and taking into account repeatability, is given:

$$\Delta C_S = \pm 0.02 C_S (20:1)$$

III. Results and Discussion

Since the major aim of this study is on side force characteristics arising from nose-induced vortex asymmetry, experimental results to be presented show primarily side force variations with incidence or Reynolds number for the different models. Following Keener et al.,[18] side force data (in most cases) are presented normalized by a base reference area, which is an equivalent area of a circle with diameter equal to the planform width at the base of the elliptic cone; however, in some of the figures concerning Reynolds number effects, it is found preferable to adopt a different area normalization, as will be specified in Sec. III.D.

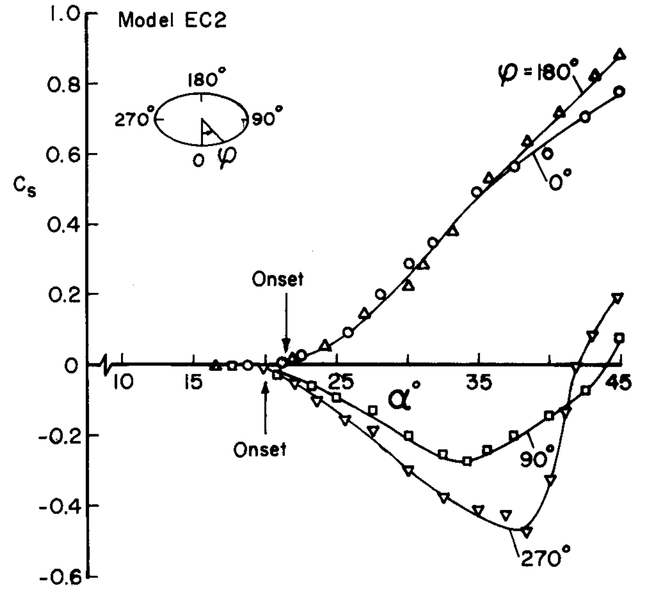

Fig. 2 Roll effects on side force: model EC2.

A. Typical Roll Effects

The importance of roll search in experimental studies of side force characteristics of axisymmetric bodies has been stressed in many earlier studies.[2,3] For a body with elliptic cross section, however, roll sensitivity can only be assessed along the two planes of symmetry. Figure 2 shows such results of side force coefficient C_S for the elliptic cone EC2 corresponding to both HE and VE orientations at a unit Reynolds number of 4.6×10^4/cm. Some differences in the side force magnitudes do exist in the symmetry planes with the angle of attack for the onset of side force unaffected for a given ellipse orientation. Based on such tests, the "regular state or stable roll" (between the symmetry planes) was identified corresponding to maximum side force magnitude for each model, and all detailed measurements were carried out at these selected roll positions. For example, φ = 180 and 270 deg were chosen as stable roll positions for model EC2 (Fig. 2), corresponding to horizontal and vertical ellipse orientations, respectively.

B. Side Force Variation with Incidence

Typical results of side force coefficient at three values of unit Reynolds number are displayed in Figs. 3–5; data for the HE and VE orientations of each model are shown separately in the figures. The following observations can be made:

1) For each model, the angle of attack for the onset side force α_0 generally depends on its orientation, while being essentially independent of Reynolds number in the range varied in the experiments. However, a small effect of Reynolds number on α_0 is seen for model EC3 with VE orientation, which is presumably due to weak crossflow separation (as revealed by surface flow features), resulting from relatively mild adverse pressure gradients in the crossflow plane compared to models EC1 and EC2.

2) Even mild ellipticity (model EC1, Fig. 3) has the effect of decreasing the value of α_0 compared to the axisymmetric counterpart, for which α_0 is given by $2\theta_c$.[2,22]

3) With an increase in the ellipticity, the maximum side force levels seem to decrease progressively for both HE and

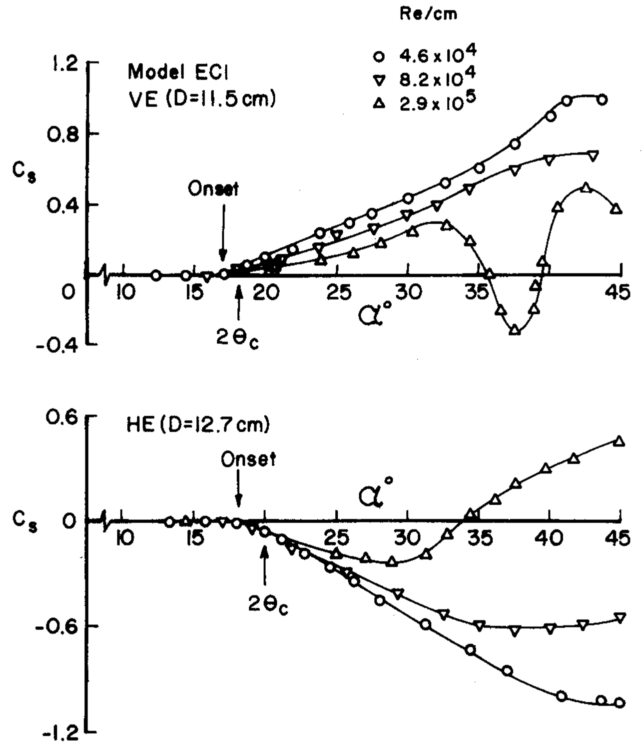

Fig. 3 Variations of side force with incidence: model EC1.

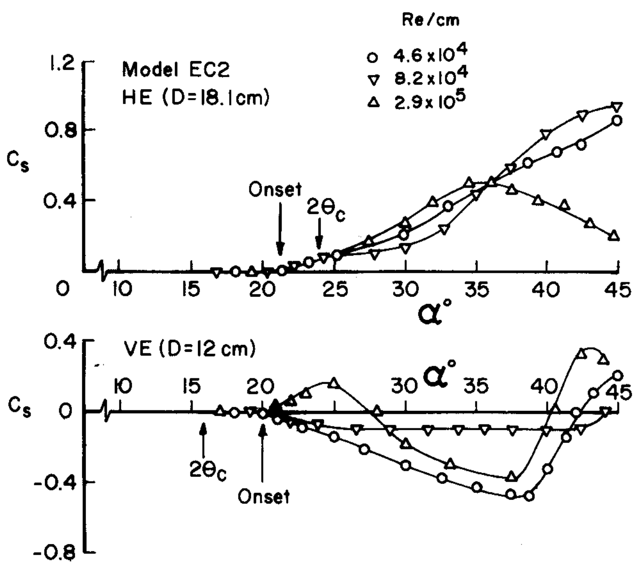

Fig. 4 Variations of side force with incidence: model EC2.

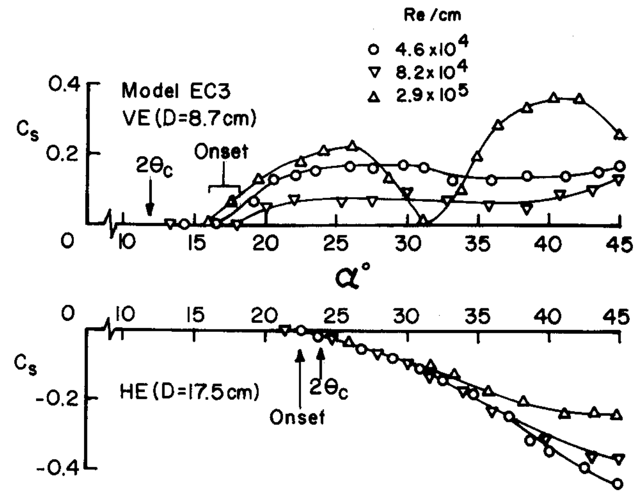

Fig. 5 Variations of side force with incidence: model EC3.

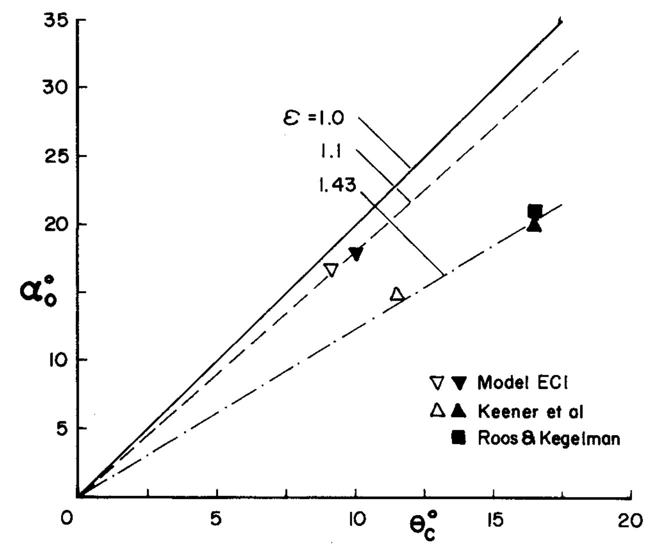

Fig. 6 Effect of ellipticity on the angle of attack for onset of side force (open and solid symbols represent vertical and horizontal ellipse orientations).

VE orientations; a detailed discussion of this aspect, including Reynolds number effects, is contained in Sec. III.D.

C. Onset of Vortex Asymmetry

Results of α_0 for the three elliptic cones in the range of Reynolds number and subsonic Mach numbers covered in the present tests are shown in two parts in Figs. 6 and 7 (the filled and unfilled symbols in these figures represent data for the horizontal and vertical ellipse orientations, respectively). The data of Keener et al.[18] and Roos and Kegelman[19] on elliptic tangent ogives have been included in Fig. 6 with the assumption that the nose shape (or equivalently the streamwise curvature) may have no influence on α_0 for a given value of ε. This assumption gets significant support from the large body of data on α_0 for axisymmetric pointed forebodies (e.g., cones, ogives, paraboloids from different tests and tunnels), which correlate well with $2\theta_c$ (see Fig. 15a, Ref. 22); the correlation[22] also suggests that geometrical model imperfections in the nose region (associated with the normal model machining/finishing procedures) may not affect α_0.

It is interesting to note from Fig. 6 that α_0 varies linearly with the appropriate θ_c, with the slope α_0/θ_c being the same for both orientations of a given elliptic cone. Also, the slope shows a progressive decrease compared to the value $\alpha_0/\theta_c \approx 2$ known for axisymmetric pointed forebodies,[2,22] indicating clearly an earlier onset for bodies with an ellipticity ratio up to 1.43. This initial trend of α_0/θ_c with ε is to be expected since there is a progressively increasing departure from axisymmetry.

With a further increase in ellipticity ratio ($\varepsilon > 1.43$), the results (Fig. 7) show a reversal in trend, namely, the onset is progressively delayed (compared to $\varepsilon \leq 1.43$) for both HE and VE orientations; further, the slopes α_0/θ_c are different for the two orientations of a given elliptic cone. This behavior is not surprising, since, for a large ellipticity ratio, a qualitative change in the crossflow features is to be expected for the two orientations. With HE orientation, an increased α_0 (even beyond $2\theta_c$) can be expected due to the increased flattening of the body cross section[23]; however, the precise limit as $\varepsilon \rightarrow \infty$ is unknown at the present time. On thin, sharp leading-edge delta wings, recent experiments[24] employing flow visualization

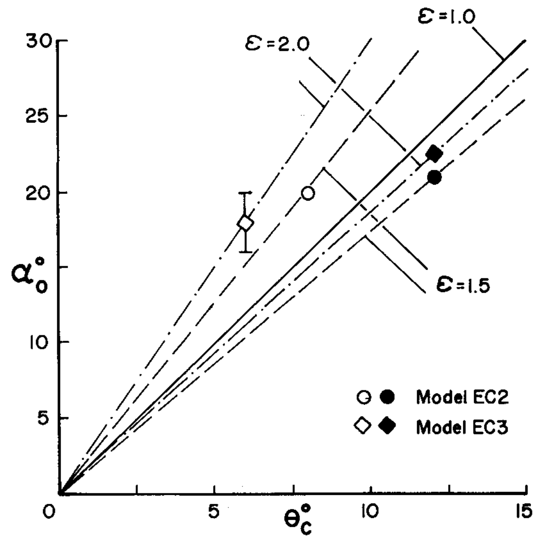

Fig. 7 Effect of ellipticity on the angle of attack for onset of side force (open and solid symbols represent vertical and horizontal ellipse orientations).

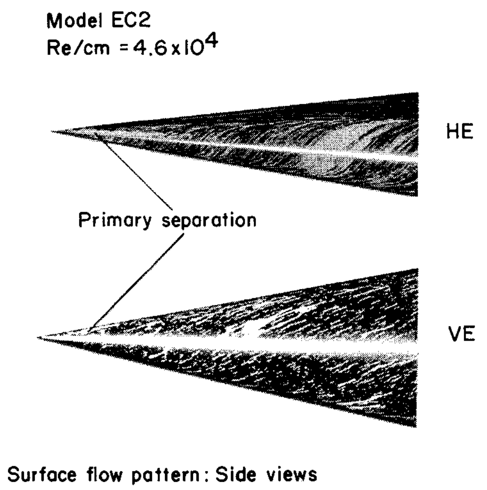

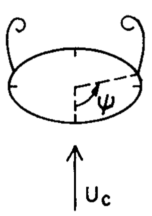

Model	λ	ψ°
EC1	1.10	115
	0.91	150
EC2	1.50	110
	0.66	160
EC3	2.00	90
	0.50	165

(Uncertainty in $\psi \simeq \pm 5°$)

Fig. 8 Some features of crossflow separation: model EC2.

studies suggest that asymmetric vortices may not occur in the absence of vortex breakdown. With VE orientation, on the other hand, we should expect the vertical flat plate limit with no crossflow separation, and hence, no vortex asymmetry.

The results presented in Fig. 6 show that α_0 depends primarily on two geometrical parameters of the forebody, namely, its nose semiapex angle and the ellipticity ratio, independent of Reynolds number (in the range $3 \times 10^5 < Re_D < 5.2 \times 10^6$) and freestream Mach number up to 0.4. These observations throw some light into the possible mechanisms that

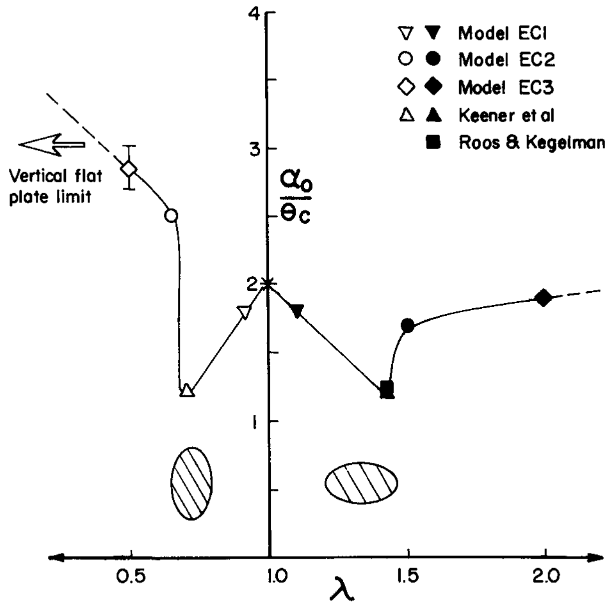

Fig. 9 Correlation of angle of attack for onset of side force on forebodies of elliptic cross section (open and solid symbols represent vertical and horizontal ellipse orientations).

may cause vortex asymmetry. Drawing an analogy with subsonic flow past a two-dimensional elliptic cylinder, it is known that the locations of the separation points for the two orientations (major axis along and normal to the flow) at any given Reynolds number are appreciably different because of widely different (streamwise) adverse pressure gradients. Similar features are observed with regard to the locations of the crossflow primary separation lines in the symmetric vortex flow regime on all three elliptic cones that are presented in Fig. 8; the data correspond to a unit Reynolds number of 4.6 × 10^4/cm and the values of ψ were obtained from surface flow visualization studies (note that the broad, white streaks in the photographs are due to the reflection of light from the camera).

In essence, for a given value of ellipticity ratio (in the range of 1–1.43), α_0 depends primarily on θ_c, independent of whether the ellipse orientation is horizontal or vertical (Fig. 6). This implies that the crossflow separation characteristics that are viscous-dominated and appreciably different for the two orientations have only a weak influence on α_0. These observations lend significant support to the hypothesis (often made in the literature) that inviscid mechanisms may play a key role in triggering asymmetry of vortex flows.

A correlation of the angle of attack for the onset of vortex asymmetry (or side forces), as influenced by the elliptic cross section, is displayed in Fig. 9. With the limited data that is available, it may be concluded that ellipticity appreciably reduces the onset (for both HE and VE orientations) up to a value of $\varepsilon = 1.43$, beyond which an increase in the value of α_0/θ_c occurs for both orientations. The data indicate a significant increase in the value of α_0/θ_c (almost three times) in the range $0.5 < \lambda < 0.7$; this arises since crossflow separation (essential for the occurrence of vortex asymmetry) rapidly weakens due to the reduced circumferential adverse pressure gradients as $\lambda \to 0$. As discussed earlier, α_0/θ_c can be expected to increase (even beyond a value of 2) for large values of λ, and additional data is needed to see this trend and also define the limiting flow for $\lambda \to \infty$.

D. Variation of Maximum Side Force with Reynolds Number

On slender bodies of circular cross section it is well known[2,3] that Reynolds number exerts a strong influence on the leeside flow structure, and hence, the side force generated. The maximum value of side force a body can generate and its depen-

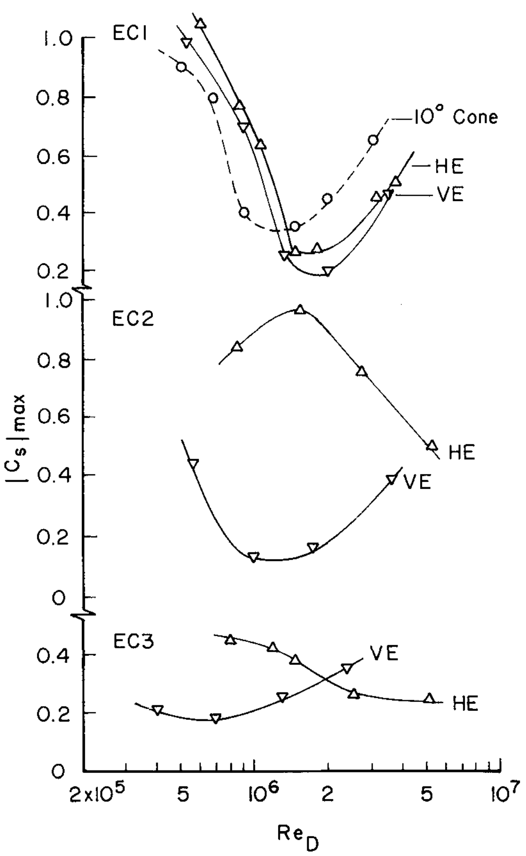

Fig. 10 Variations of (maximum) side force coefficient with Reynolds number.

dence on Reynolds number have been of great interest,[25] both from the point of view of general understanding as well as in design applications.

Based on all the tests on each model, the maximum (absolute) value of side force generated at different Reynolds numbers is shown plotted in Fig. 10. Results for a 10-deg semiapex angle circular cone[26] (tested in the same tunnel as the present experiments) are included along with the data on model EC1 in the figure for comparison. As one may expect, the results for the mildly elliptic cone are similar to those for the circular cone both with regard to the side force magnitude as well as the trend with Reynolds number. Interestingly, on the model EC2 ($\varepsilon = 1.5$), the maximum and minimum values of $|C_S|_{\max}$ are generated for the HE and VE orientations, respectively, in what appears to be a transitional range of Reynolds number.[2,17] The maximum side force characteristics on the model EC3 ($\varepsilon = 2.0$) shows reduced magnitude for both HE and VE orientations (compared to its counterpart on the model EC2); further, the data indicate a much weaker dependence on Reynolds number, which is consistent with the expected crossflow features for large ε, discussed in Sec. III.C.

Two features in the results presented earlier (Fig. 10) are striking. First, the horizontal or flattened ellipse generates relatively higher side force levels compared to VE orientations (e.g., models EC2, EC3)—this aspect is further discussed later. Second, the model EC2 with horizontal ellipse orientation generates the highest side force in the transitional range of Reynolds number. Similar trends of side force characteristics for the elliptic tangent ogive ($\varepsilon = 1.43$) were observed by Keener et al.[18] and were discussed by Hunt in his review.[2] Both of the previous features are obviously a result of the complex asymmetric (leeside) flow structure for the HE orientation. Figure 11 presents the leeside surface flow pattern

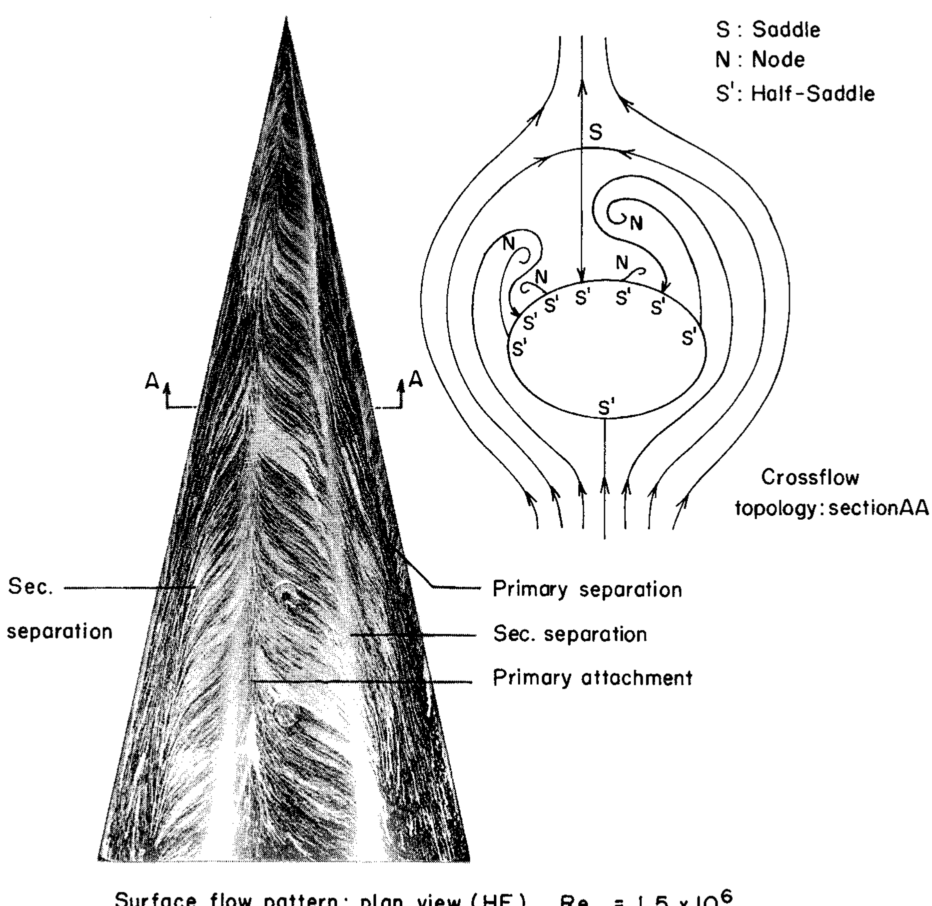

Fig. 11 Surface flow pattern and crossflow topology on model EC2: alpha = 45 deg.

and the associated crossflow topology for the model EC2 at the maximum side force condition. The vortex footprints reveal significant asymmetry of the primary attachment line and secondary separation lines; the side views (photographs not shown) indicated asymmetry of primary separation lines with $\Delta\Psi \approx 10$ deg. This observed trend of (maximum) side force for the HE is unexpected and surprising since asymmetry in crossflow separation lines can be expected to be small (because of strong circumferential adverse pressure gradients for the HE orientation), and further, the side area on which vortex asymmetry effects can act is smaller than for the VE orientation. The higher side force magnitude presumably results from the increased strength of crossflow vortices (associated with higher velocities along crossflow separation lines for the HE orientation) so that even mild or weak asymmetry in primary separation lines is amplified in terms of differential surface pressures across the (vertical) plane of symmetry.

Reding and Ericsson[25] have suggested that it may be more appropriate to display the results of maximum side force normalized by the normal force coefficient C_N corresponding to $|C_S|_{max}$. The data in Fig. 10 are therefore replotted in terms of $|C_S|_{max}/C_N$ against Re_D in Fig. 12. It may be observed that the basic trends with Reynolds number on the three cones are unaltered, but for a vertical shift in the side force magnitude depending on the C_N values.

Finally, with a view to assessing the true effect of body cross section in the generation of maximum side force, the side force data nondimensionalized by the appropriate side areas (for the two orientations of the elliptic cone) are presented against Reynolds number in Fig. 13. The higher side force levels generated by the horizontal ellipse orientation are once again brought out clearly; further, the data (on models EC2 and EC3) indicate rapidly diminishing effects of asymmetry for the VE orientation for $\lambda < 0.7$.

To summarize, the results of maximum side force characteristics (Fig. 13) and of vortex asymmetry onset (Figs. 6 and 9) lead us to the broad conclusion that a pointed forebody with a flattened ellipse (or ellipse-like) cross section results in an earlier onset (in comparison with the axisymmetric counterpart) and generates sizeable levels of side force for $\lambda \lesssim 1.5$. In light of these results, it would appear that the aerodynamic benefits of the F-5 aircraft forebody[13] result from its blunt nose in planform (i.e., large θ_c) leading to a significantly delayed onset of asymmetry and excellent optimization of forebody/wing/ LEX geometries for improved high-alpha characteristics. An early conjecture along these lines was made by Polhamus[17] based on the limited data of Keener et al.[18]

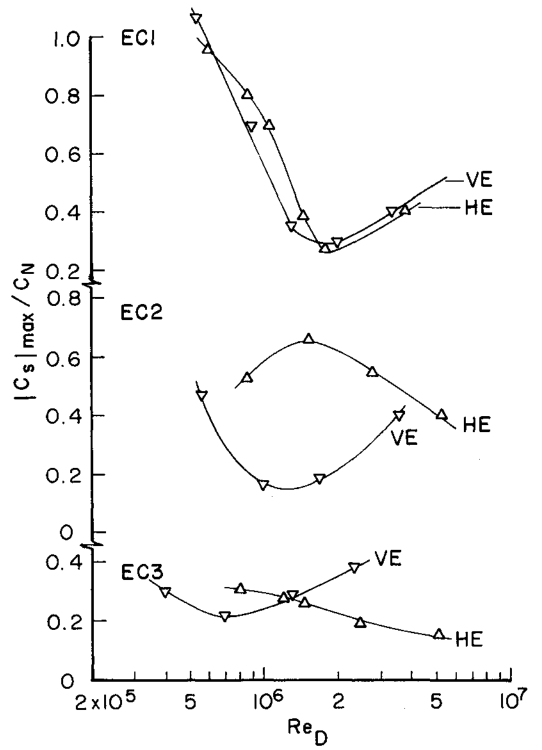

Fig. 12 Variations of normalized (maximum) side force coefficient with Reynolds number.

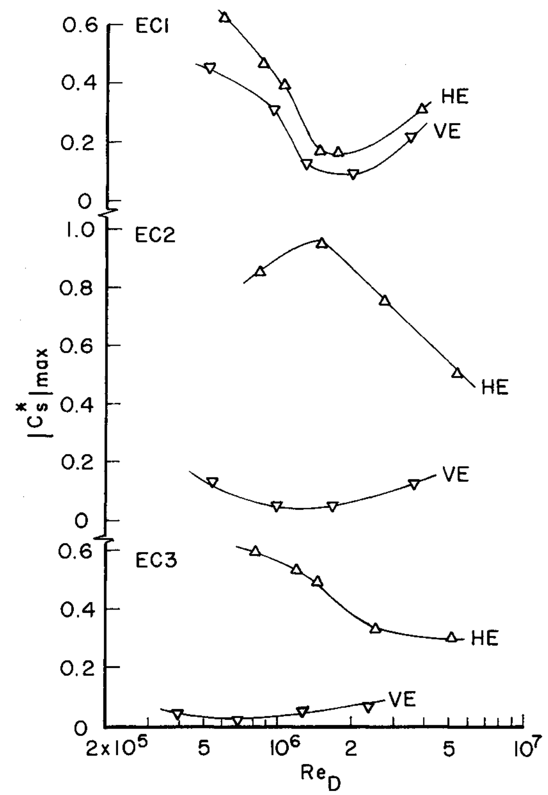

Fig. 13 Variations of (maximum) side force coefficient (based on side area) with Reynolds number.

E. Effect of Mach Number

Certain broad effects of Mach number on the onset of asymmetry and maximum side force magnitudes are now reasonably well known in the context of forebodies with a circular cross section.[2,3] These include a delayed onset and a significant reduction in the maximum side force generated that are linked to crossflow compressibility effects, including the appearance of shock waves. As stated in Sec. II, measurements at higher speeds (in the present series of tests) were made at Mach numbers of 0.6 and 0.8; the corresponding unit Reynolds numbers (per cm) were 0.20 and 0.24 × 10^6, respectively.

Figure 14 presents results of side force coefficient on all three models corresponding to both HE and VE orientations. The following observations can be made with the limited data displayed:

1) On models EC1 and EC2, the values of α_0 at $M_\infty = 0.6$ are essentially the same as those observed at lower speeds (Figs. 3 and 4) for both ellipse orientations, while the onset is slightly delayed (about 1–2 deg) at $M_\infty = 0.8$.

2) On the model EC3, on the other hand, the data for the horizontal ellipse exhibits a significantly delayed onset with Mach number (about 18 deg at $M_\infty = 0.8$), presumably caused by crossflow compressibility effects; a similar, but much weaker trend is seen for the VE orientation.

3) With regard to maximum side force magnitudes, they are generally lower compared to the (appropriate) values measured at lower speeds (Fig. 10).

To summarize, the general trends involving a delay in the onset of asymmetry and reduced levels of (maximum) side

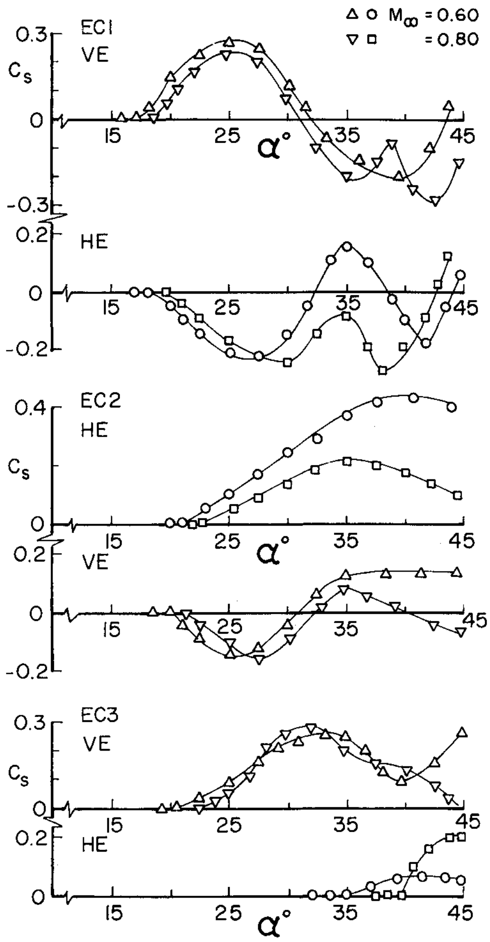

Fig. 14 Effect of Mach number on the angle of attack for onset of side force.

force magnitude with increase in Mach number are broadly similar to the characteristics known for bodies of revolution.[2,3]

IV. Conclusions

To gain understanding of some of the main features of vortex asymmetry and associated side forces on pointed forebodies of elliptic cross section, a systematic experimental study involving a family of three elliptic cones was undertaken. Results show that, for both horizontal as well as vertical orientations of the ellipse, ellipticity progressively reduces the angle of attack for the onset of side force (compared to the axisymmetric case) up to an ellipticity ratio ε of 1.43, beyond which there is a reversal in this trend; this reversal in the vortex asymmetry onset is due to a qualitative change in the nature of crossflow features for the two orientations for large ε. A correlation of the angle of attack for the onset of vortex asymmetry, involving the (appropriate) planform nose semi-apex angle and the ratio of planform width-to-height of the ellipse λ is suggested. These results provide strong support to the hypothesis (often made in the literature) that inviscid mechanisms may play a key role in triggering asymmetry of vortex flows.

With regard to the maximum side force generated, it is appreciably higher for the horizontal (compared to the vertical) ellipse orientation on each model. For $\lambda \gtrsim 1.43$, the trend of the available data suggests that the (maximum) side force generated may actually decrease at the higher Reynolds numbers, which is a desirable feature in applications. For the vertical ellipse orientation, a drastic reduction in the (maximum) side force magnitude is observed for $\lambda < 0.70$.

Finally, there is a need to generate additional data on pointed forebodies with elliptic cross section (e.g., cones, ogives with different values of nose apex angle, ellipticity ratio) at much higher Reynolds numbers to assess the validity of the correlation for the onset of asymmetry suggested here and to establish some of the broad trends observed with regard to the (maximum) side force generated with Reynolds number. It is also of significant interest to establish the limiting flow for $\lambda \to \infty$.

Acknowledgments

The author expresses his sincere thanks to K. Y. Narayan for his early association with the project and for many interesting discussions during the course of this work. Thanks are due to Lewis Schiff and Murray Tobak of NASA Ames Research Center for fruitful discussions on some aspects of the results presented here. Finally, the service and assistance rendered by the staff of the model shop in model fabrication and the 1.2-m tunnel during the tests are gratefully acknowledged.

References

[1]Ericsson, L. E., and Reding, J. P., "Vortex Induced Asymmetric Loads in 2-D and 3-D Flows," AIAA Paper 80-0181, Jan. 1980.

[2]Hunt, B. L., "Asymmetric Vortex Forces and Wakes on Slender Bodies," AIAA Paper 82-1336, Aug. 1982.

[3]Ericsson, L. E., and Reding, J. P., "Asymmetric Flow Separation and Vortex Shedding on Bodies of Revolution," *Tactical Missile Aerodynamics*, edited by M. J. Hemsch, Vol. 141, Progress in Astronautics and Aeronautics, AIAA, Washington, DC, 1992, pp. 391–452.

[4]Keener, E. R., and Chapman, G. T., "Similarity in Vortex Asymmetries over Slender Bodies and Wings," *AIAA Journal*, Vol. 15, No. 9, 1977, pp. 1370–1372.

[5]Dyer, D. E., Fiddes, S. P., and Smith, J. H. B., "Asymmetric Vortex Formation from Cones at Incidence; A Simple Inviscid Model," *Aeronautical Quarterly*, Vol. 33, Pt. 4, 1982, pp. 293–312.

[6]Fiddes, S. P., and Smith, J. H. B., "Asymptotic Separation from Slender Cones at Incidence," *Proceedings of the IUTAM Symposium on Boundary Layer Separation*, edited by F. T. Smith and S. N. Brown, Springer–Verlag, Berlin, 1987, pp. 363–375.

[7]Degani, D., and Schiff, L. B., "Numerical Simulation of the Effect of Spatial Disturbances on Vortex Asymmetry," *AIAA Journal*, Vol. 29, No. 3, 1991, pp. 343–352.

[8]Degani, D., "Effect of Geometrical Disturbance on Vortex Asymmetry," *AIAA Journal*, Vol. 29, No. 4, 1991, pp. 560–566.

[9]Degani, D., and Levy, Y., "Asymmetric Turbulent Vortical Flows over Slender Bodies," *AIAA Journal*, Vol. 30, No. 9, 1992, pp. 2267–2273.

[10]Chambers, J., "High-Angle-of-Attack Aerodynamics: Lessons Learned," AIAA Paper 86-1774, June 1986.

[11]Ericsson, L. E., "Sources of High Alpha Vortex Asymmetry at Zero Side-Slip," *Journal of Aircraft*, Vol. 29, No. 6, 1992, pp. 1086–1090.

[12]Ericsson, L. E., "Some Thoughts on Conical Flow Asymmetry," AIAA Paper 92-0427, Jan. 1992.

[13]Skow, A. M., and Ericsson, G. E., "Modern Fighter Aircraft Design for High Angle of Attack," AGARD Lecture Series no. 121, High Angle of Attack Aerodynamics, March 1992.

[14]Graves, E. B., "Aerodynamic Characteristics of a Monoplanar Missile Concept with Bodies of Circular and Elliptical Cross Sections," NASA TM-74079, Dec. 1977.

[15]Jackson, C. M., Jr., and Sawyer, W. C., "Bodies with Non-Circular Cross Sections and Bank-to-Turn Missiles," *Tactical Missile Aerodynamics*, edited by M. J. Hemsch, Vol. 141, Progress in Astronautics and Aeronautics, AIAA, Washington, DC, 1992, pp. 365–389.

[16]Brandon, J. M., and Nguyen, L. T., "Experimental Study of Effects of Forebody Geometry on High Angles of Attack Static and Dynamic Stability," AIAA Paper 86-0331, Jan. 1986.

[17]Polhamus, E. C., "A Review of Some Reynolds Number Effects Related to Bodies at High Angles of Attack," NASA CR 3809, Aug. 1984.

[18]Keener, E. R., Chapman, G. T., Cohen, L., and Taleghani, J., "Side Forces on Forebodies at High Angles of Attack and Mach Numbers from 0.1 to 0.7—Two Tangent Ogives, Paraboloid and Cone," NASA TMX-3438, Feb. 1977.

[19]Roos, F., and Kegelman, J. T., "Aerodynamic Characteristics of Three Generic Forebodies at High Angles of Attack," AIAA Paper

91-0275, Jan. 1991.

[20]Lowson, M. V., and Ponton, A. J. C., "Symmetric and Asymmetric Vortex Flows at High Angles of Attack," AIAA Paper 91-0276, Jan. 1991.

[21]Kline, S. J., and McClintock, F. A., "Describing Uncertainties in Single Sample Experiments," *Mechanical Engineering*, Vol. 75, No. 1, 1953, pp. 3–8.

[22]Keener, E. R., and Chapman, G. T., "Onset of Aerodynamic Side Forces at Zero Sideslip on Symmetric Forebodies at High Angles of Attack," AIAA Paper 74-770, Aug. 1974.

[23]Stahl, W. H., "Experimental Investigations of Asymmetric Vortex Flows Behind Elliptic Cones at Incidence," *AIAA Journal*, Vol. 31, No. 5, 1993, pp. 966–968.

[24]Stahl, W. H., Mahmood, M., and Asghar, A., "Experimental Investigation of the Vortex Flow on Delta Wings at High Incidence," *AIAA Journal*, Vol. 30, No. 4, 1992, pp. 1027–1032.

[25]Reding, J. P., and Ericsson, L. E., "Re-Examination of the Maximum Normalised Vortex–Induced Side Force," *Journal of Spacecraft*, Vol. 21, No. 5, 1984, pp. 433–440.

[26]Viswanath, P. R., and Narayan, K. Y., "Side Force Characteristics of a 20 Deg. Cone at High Angles of Attack," National Aerospace Labs., NAL TM AE 8503, May 1985.